Above-Threshold Ionization of Quasiperiodic Structures by Low-Frequency Laser Fields

F. Catoire* and H. Bachau†
Centre des Lasers Intenses et Applications, CNRS-CEA-Université de Bordeaux, 351 Cours de la Libération, Talence F-33405, France
(Received 21 March 2015; published 15 October 2015)

We investigate the theoretical problem of the photoelectron cutoff change in periodical structures induced by an infrared laser field. We use a one-dimensional Kronig-Penney potential including a finite number of wells, and the analysis is fulfilled by resolving the time-dependent Schrödinger equation. The electron spectra, calculated for an increasing number of wells, clearly show that a plateau quickly appears as the periodic nature of the potential builds up, even at a moderate intensity (10 TW/cm^2). Varying the intensity from 10 to 30 TW/cm^2 we observe a net increase of both the yield and accessible energy range of the ionization spectrum. In order to gain insight into the dynamics of the system at these intensities, we use an analytical approach, based on exact solutions of the full Hamiltonian in a periodic potential. We show that the population transfers efficiently from lower to upper bands when the Bloch and laser frequencies become comparable. The model leads to a quantitative prediction of the intensity range where ionization enters the nonperturbative regime. Moreover, it reveals the physics underlying the increase of the photoelectron energy cutoff at moderate intensities, as observed experimentally.

DOI: 10.1103/PhysRevLett.115.163602 PACS numbers: 42.50.Hz, 32.80.Wr, 36.40.-c, 79.60.-i

When an atom is submitted to an intense and short laser field it gives rise to nonlinear effects such as high-order harmonic generation (HHG) [1] or above-threshold ionization (ATI) [2]. Over the past two decades, HHG from noble gases has become a practical source of ultrashort pulses in the UV and extreme ultraviolet domains (see Refs. [3,4] for reviews). HHG resulting from a high intensity laser interacting with atoms is well described by the semiclassical three-step model, called the simple man model [5–8]. This model predicts the single-atom or small molecule maximum photon energy of the harmonic spectrum at $I_p + 3.2U_p$ where I_p is the ionization potential of the atom. U_p is the ponderomotive energy of the electron in the laser field ($U_p = (I/4\omega^2)$, where I is the peak intensity and ω is the laser frequency, expressed in a.u.) when linearly polarized light is used. Regarding ATI in atoms, the above cited three-step model also predicts the electron energy distribution. ATI spectra can be described by a combination of direct and rescattering (indirect) ionization processes. The maximum electron kinetic energy for direct and rescattering processes are $2U_p$ and $10U_p$, respectively. Experimentally, both HHG and ATI high-energy spectra exhibit a structure called the plateau with the expected cutoff in agreement with theoretical predictions [9–13]. Alternatively, HHG spectra generated in a bulk crystal show a plateau cutoff that scales linearly with the electric field amplitude of the drive laser. In order to explain this behavior, a different mechanism than the usual three-step model has been suggested involving a classical field-driven Bloch oscillation dynamics [14,15]. Similarly, ATI spectra in semiconductors show a wide plateau with high energy electrons, having a cutoff that is much more extended than the $10U_p$ limit observed in atoms. A typical example is given in Ref. [16] where the CsI crystal irradiated by an 800 nm femtosecond laser at 3 TW/cm^2 shows a cutoff at 124 U_p (24 eV). It is worth noting that a similar trend exists for other crystals [17], showing the universality of the process. The heating was generally considered as a result of a cascade of phonon-assisted photon absorption in the conduction band (e.g., Ref. [18]) but this process explains only the peak in the low energy range (up to a few eV) of the spectrum [19]. Resolving the time-dependent Schrödinger equation (TDSE) in the basis of Bloch functions in the conduction band, we have been able to show that the electron transfer from one band to the upper ones is already effective at intensities of a few terawatts (TW) [20]. Nevertheless the physical mechanism underlying these transitions remains unclear. More generally, it is of crucial interest to clarify, as has been done in the case of atoms and molecules, the relevant parameters governing the transition from perturbative to nonperturbative behavior in the ionization of quasiperiodic and periodic structures submitted to low-frequency laser fields. In order to have a better insight into the role of the periodicity of the system in ATI spectra we use a multiwell potential with one active electron, an approach that has been used to model a wide number of physical systems (see Ref. [21], and references therein). Atomic units are used throughout the Letter unless stated otherwise.

We use a one-dimensional potential $V(x)$ composed of N wells defined as follows

$$V(x) = -U_0 \tag{1}$$

for $na-(b/2)\leq x\leq na+(b/2)$ and $V(x)=0$ elsewhere. Here $n=-N/2,\ldots,-1,1,\ldots,N/2$, and for $N=\infty$ one recognizes the Kronig-Penney model with rectangular potentials of width b separated by a distance a, which is the lattice period. The total number of wells involved in the potential is N, which is chosen even for symmetry properties of the potential imposed by the boundaries of the numerical box. We choose $b=\frac{3}{4}a$, $a=8.6$ a.u., and $U_0=0.015$ a.u. in order to mimic the CsI crystal band structure [20]. The corresponding band energy diagram, calculated for $N=\infty$, is given in Fig. 1. We consider the time evolution of an electron under the influence of an electromagnetic field linearly polarized. The TDSE may be written, in the Coulomb gauge and dipole approximation,

$$H\Psi(x,t)=\left\{\frac{[P+A(t)]^2}{2}+V(x)\right\}\Psi=i\frac{\partial\Psi}{\partial t}. \quad (2)$$

P is the electron momentum operator. $A(t)$ is the electromagnetic field vector potential of central pulsation ω and amplitude E_0/ω. The potential vector is chosen so that $A(t=0)=A(T)=0$, with T the end of the pulse. Thus, the relation $A(T)=-\int_0^T dtE(t)=0$ [where $E(t)$ is the electric field] is satisfied, ensuring that there is no static field component that could lead to any problem related to gauge invariance [22]. The TDSE is solved numerically. The initial state (at $t=0$) is the eigenstate of lowest eigenenergy of the Hamiltonian H with no field. This wave function has a momentum distribution centered at $k=0$ and a negative eigenenergy, close to 0. The split-operator and the Crank-Nicolson methods are used to evaluate the evolution operator; the numerical convergence is checked using the usual procedure, i.e., by varying the grid parameters. Once the wave function has been calculated at the end of the pulse, the photoelectron spectrum is extracted by using the so-called resolvent method (see Ref. [23] and references therein). It is worth recalling that the TDSE includes intraband and interband transitions, as well as (ac) Stark shifts, which slightly distort the bands at 10 TW/cm^2 [20].

We first plot the ionization density probability as a function of the number of wells. The results are presented in Fig. 2. In the case where one well is involved (i.e., corresponding to the atomic case) we clearly observe a series of ATI peaks of decreasing magnitude, followed by a change of slope and a cutoff at about $10U_p$ (6–7 eV). The Keldysh parameter $\gamma=\sqrt{I_p/2U_p}$ [24] (we recall that I_p is the atomic ionization potential) is smaller than 1 ($\gamma=0.24$) indicating that the physics is deeply in the so-called tunneling regime.

When the number of wells is increased, a clear change of the photoelectron spectrum is observed: a first plateau with a cutoff at about 7 eV is observed, followed by a second plateau with a cutoff at about 50 U_p (30 eV). The periodicity condition, for a given energy range, is numerically checked by increasing N until convergence of the ionization density probability. For example, in the energy region up to 35 eV, a saturation (i.e., a convergence) of the ionization density probability is observed when the number of wells goes over $N=10$. This means that for this energy range, the Brillouin zone involved in the physics is equivalent to having an infinite number of wells. Narrower structures show up in the photoelectron spectrum

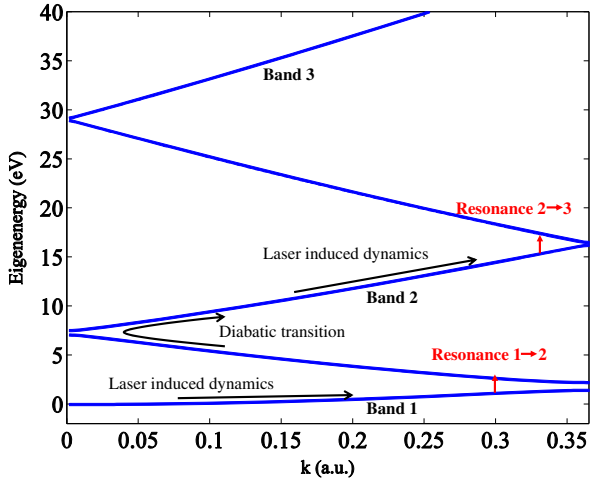

FIG. 1 (color online). Plot of the band diagram corresponding to half of the first Brillouin zone $k=[0,\pi/a]$, assuming the Kronig-Penney potential defined in the text and an infinite number of wells. Note that the interval defined by $k=[-\pi/a,0]$ is simply the symmetric representation of $k=[0,\pi/a]$.

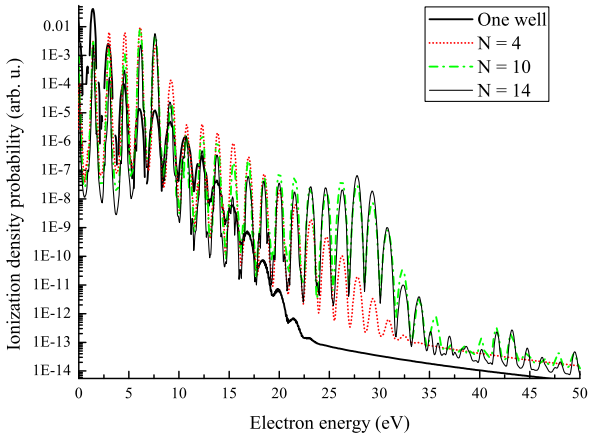

FIG. 2 (color online). Plot of the density probability as a function of the electron energy for various number N of wells. The laser parameters are an intensity of $I=10$ TW/cm^2, a central wavelength of 800 nm, and a pulse duration of 20 fs FWHM using a $\sin^2$ envelope. The ponderomotive energy is $U_p=0.6$ eV. The one well case has been calculated for 10 fs FWHM and a potential width of twice the one for the multiwell case in order to get similar ionization yield.

at larger energies. These features are better contrasted in Fig. 3 (indicated by arrows) at higher intensities for reasons that will be explained later. The figure shows the photoelectron spectrum density probability for different intensities with a fixed number of wells ($N = 14$). We have verified that, for $N = 14$, the condition of periodicity is reached over the energy range of 0–108 eV. In this graph a clear breakup of the classical $10U_p$ cutoff is observed for intensities higher than $I = 3$ TW/cm^2. For example, at 30 TW/cm^2 ($U_p \approx 1.9$ eV), peaks are observed at 7.7, 29.2, 65.5, and 96.6 eV. This confirms that a critical intensity exists above which the ATI spectrum shows a nonperturbative behavior. The narrow peaks are related to the Bragg diffraction (corresponding to the crossing point of the energy diagram at $k = 0$ in Fig. 1); in other words they result from the coherent contribution of the different centers and are defined at the energy positions $E_n = (2\pi^2/a^2)n^2$ $(n = 1, 2, \ldots)$. This leads to peaks expected at $E_n(\text{eV}) \approx 7.26n^2$, in close agreement with the spectrum of Fig. 3 (except for the structure of very low magnitude at 96.6 eV). Incidentally, it is worth noting that the effect of the spatial dependence of the intensity should not affect the presence of Bragg peaks since they are independent of I.

In order to explain the physics underlying the evolution of the spectra in the range 10–30 TW/cm^2 we present below a theoretical approach, derived from Ref. [25], based on few state expansion and leading to simple analytical expressions of the transition amplitudes. We obtain $\Psi(x, t)$ from $\Psi(x, 0)$ by employing an eigenfunction expansion whose components are solutions of

$$H\Phi_i(x, t) = \epsilon_i(t)\Phi_i(x, t). \tag{3}$$

$\epsilon_i(t) \equiv \epsilon_i(k(t))$ where $\epsilon_i(k)$ is the energy band solution of the central equation as depicted in Fig. 1. $k(t)$ is the electron momentum. Its dependence with t is deduced from the requirement of periodic boundary conditions [25,26]. This leads, in agreement with the classical equation of motion, to

$$\frac{dk(t)}{dt} = \frac{d\mathrm{A}(t)}{dt} = -E(t) \tag{4}$$

and

$$k(t) - A(t) = k(t = 0). \tag{5}$$

$A(t) = -(E_0/\omega)\sin\omega t$ and $E(t)$ defines the electric field vector of amplitude E_0.

We now consider the perturbative transition from dressed band l to dressed band m defined in Eq. (3). The first order perturbation theory, applied on the dressed states, gives rise to the amplitude transition $t_{m,l}$ expressed as

$$t_{m,l}(t) \sim \int_0^t dt' p_{ml}(k(t'))e^{iS(t')},$$
$$\text{where } S(t') = \int_0^{t'} [\epsilon_m(k(t'')) - \epsilon_l(k(t'')) \pm \omega]dt''. \tag{6}$$

$p_{ml}(k(t'))$ is the matrix element of the operator P between the bands m and l at time t'. We consider first the case of the transition from band 1 to band 2 with the calculation of $t_{2,1}(t)$. In agreement with the TDSE calculations we assume that initially (i.e., at $t = 0$) the population is in band 1 and centered at $k = 0$. From Eq. (6) it is clear that the transition efficiency relies on the stationarity of the phase condition of the integrand. Thus, we look at the values of $k_r = k(t_r)$ satisfying the condition $(\partial S/\partial t)_{t=t_r} = 0$, which is

$$\epsilon_2(k_r) - \epsilon_1(k_r) - \omega = 0, \tag{7}$$

hereafter called the resonance condition. The evaluation of k_r requires the knowledge of the dispersion functions $\epsilon_2(k)$ and $\epsilon_1(k)$ within the first Brillouin zone. In our example k_r can be deduced from Fig. 1, where the resonance position k_r is indicated by the lower red arrow. Then, if we consider that $k(t = 0) = 0$, the relation $k_r = -(E_0/\omega)\sin\omega t_r$ deduced from Eq. (5) shows that the resonance condition is periodically fulfilled provided that the field amplitude satisfies $E_0 \geq k_r\omega$. In our case this leads to a minimum intensity of 9 TW/cm^2. Considering now the transition from band 2 to band 3, the transition amplitude is maximum for $\epsilon_3(k'_r) - \epsilon_2(k'_r) - \omega = 0$ (k'_r is indicated by the upper red arrow in Fig. 1). This is realized for a minimum intensity of 13 TW/cm^2. Incidentally, we note that this value of the intensity also ensures an efficient transfer from band 1 to band 2. It must be also noted that once a part of the wave function reaches the crossing point at $k = 0$, a diabatic transition occurs due to the velocity

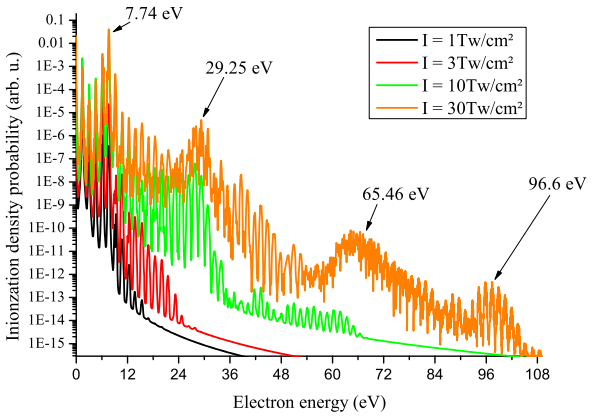

FIG. 3 (color online). Plot of the density probability as a function of the electron energy for different peak intensity (I). The laser parameters are a central wavelength of 800 nm and a pulse duration of 20 fs using a sin^2 envelope. The number of well is fixed at $N = 14$.

acquired by the wave packet during the interaction with the laser pulse, as indicated by the curved arrow in Fig. 1. As a matter of fact the population oscillates within the whole Brillouin zone $[-\pi/a, \pi/a]$ under the action of the field. We only show half of the first Brillouin zone in Fig. 1; a mirror process manifests for negative values of k. The generalization to transitions between upper bands is straightforward. One can easily show that, when k_r reaches the limit of the Brillouin zone, i.e., $k_r = \pm\pi/a$, the resonance condition is always fulfilled (the successive bands are quasidegenerate at the limits of the Brillouin zone). According to the relation $k_r = -(E_0/\omega)\sin\omega t_r$ the latter equality requires $E_0 \geq k_r\omega$ to be fulfilled, or introducing the Bloch frequency $\omega_b = aE_0$, this condition is written $\omega_b \geq \pi\omega$. In our particular case, this is realized for a minimum intensity of 14 TW/cm^2. For $I \geq 14$ TW/cm^2 the electron can "jump" from band 1 to any upper band through successive transitions, occurring at different times, i.e., each time the resonance condition $\epsilon_m(k_r) - \epsilon_l(k_r) \pm \omega = 0$ is realized. These considerations fully agree with the results of the TDSE calculations shown in Fig. 3 where a net increase of ionization yield over a large range of electron energies for intensities ranging from 10 to 30 TW/cm^2 is observed. We have checked that, increasing the intensity from 10 to 20 TW/cm^2, the peaks associated with the population in bands 2, 3, and 4 appear successively. At 30 TW/cm^2 the whole spectrum is populated and all peaks are clearly pronounced (see Fig. 3).

We are now able to give a physical picture of the process. First, we recall that ω_b, the Bloch frequency, refers to the oscillation of the electron within the Brillouin zone under the action of a static electric field E_0 [27,28]. When the field intensity reaches the value of 9 TW/cm^2, band 2 is populated according to the scheme shown in Fig. 1. Increasing the intensity, bands 3 and 4 are populated following a similar scheme. For an intensity of 14 TW/cm^2, k reaches the limit $\pm\pi/a$ of the Brillouin zone, and we enter in a complex ionization regime where the wave packet dynamics undergoes Bloch oscillations within the bands while the laser field varies slowly. At the same time the population transfers efficiently from one band to another close to the limits of the Brillouin zone. Somehow one can make a parallel with the case of tunnel (nonperturbative) ionization in atoms, which is expected to dominate when $\gamma < 1$, i.e., a situation of tunnel ionization in a quasistatic field. In the case of quasiperiodic systems, we have shown that the physics of ionization is governed by the ratio of the field frequency over the Bloch frequency ω/ω_b, which indicates the limit between the perturbative and nonperturbative regime. The latter becomes dominant when $\omega/\omega_b < 1$. Note that in the limit of a static field ($\omega = 0$) the situation tends to the nonperturbative tunneling described by the seminal paper of Zener [29]. As a matter of fact, for intensities larger than few tens of TW/cm^2 interband couplings become stronger and the analytic treatment leading to the transition amplitude (6) should be carefully considered. Indeed, the approach leading to Eq. (6) is nonperturbative in the sense that it relies on the exact treatment of each Bloch function in the electromagnetic field [Eq. (3)], but the interband coupling is treated perturbatively.

In conclusion, we have uncovered an efficient mechanism that populates the bands of a quasiperiodic potential; it overtakes perturbative multiphoton ionization when the Bloch frequency ω_b satisfies $\omega_b \approx \pi\omega$. This directly leads to a simple quantitative evaluation of the minimum intensity required for an efficient population transfer between the lower (initially populated) band to the upper ones. In our case ($a = 8.6$ a.u.), this mechanism is predicted at the rather low intensity of 9 TW/cm^2. This is in full agreement with the TDSE calculations, which show a rich ATI spectrum for intensities of the order of 10–30 TW/cm^2, with electron peaks well identified up to $50U_p$, well above the cutoff predicted by classical models in atoms. Furthermore, given the simplicity of the 1D model, one can consider that the comparison with the experiment evoked in the introduction (which shows at 3 TW/cm^2 an electron spectrum dominated by a broad and high structure at low energy, followed by a plateau with a cutoff at 24 eV [16]) is reasonably good. Indeed, the density of states in the conduction band decreases with energy as $E^{-1/2}$ in 1D while it increases like $E^{1/2}$ in 3D, making the absorption of photons more efficient in the latter case [17]. Note that, in 3D, other factors like the orientation of the crystal with respect to the laser field polarization should be taken into account since the lattice periodicity varies with the direction considered in the crystal, thus influencing the position of the Bragg structures. Besides quantitative predictions, the model gives a clear insight into the physics underlying the ATI process: under the action of the electromagnetic field, the electron gains momentum along a band and "jumps" to an upper one, close in energy, when it reaches the limit of the Brillouin zone. In addition, with the recent work on HHG evoked in the introduction, our findings confirm that the field driven oscillations along the bands play a crucial role in nonlinear processes and that the Bloch frequency is a key parameter in this context. This is of prime interest to understand the behavior of complex systems involving a finite number of potential wells, like clusters or nanostructures submitted to TW-IR fields, in which the properties presented in this work are then expected to appear.

The authors would like to thank P. Martin, A. Vasil'ev, and J. C. Delagne for fruitful discussions. Computer time for this study was provided by the computing facility MCIA (Mésocentre de Calcul Intensif Aquitain) of the Université de Bordeaux and of the Université de Pau et des Pays de l'Adour. We also acknowledge financial support from the Centre National de la Recherche Scientifique (PICS No. 36934).

*catoire@celia.u-bordeaux1.fr
†bachau@celia.u-bordeaux1.fr

[1] G. H. C. New and J. F. Ward, Phys. Rev. Lett. **19**, 556 (1967).
[2] P. Agostini, F. Fabre, G. Mainfray, G. Petite, and N. K. Rahman, Phys. Rev. Lett. **42**, 1127 (1979).
[3] T. Brabec and F. Krausz, Rev. Mod. Phys. **72**, 545 (2000).
[4] F. Krausz and M. Ivanov, Rev. Mod. Phys. **81**, 163 (2009).
[5] T. F. Gallagher, Phys. Rev. Lett. **61**, 2304 (1988).
[6] H. B. van Linden van den Heuvell and H. G. Muller, *in Multiphoton Processes*, Cambridge Studies in Modern Optics Vol. 8, edited by S. J. Smith and P. L. Knight (Cambridge University Press, Cambridge, England, 1988).
[7] K. J. Schafer, B. Yang, L. F. DiMauro, and K. C. Kulander, Phys. Rev. Lett. **70**, 1599 (1993).
[8] P. B. Corkum, Phys. Rev. Lett. **71**, 1994 (1993).
[9] J. J. Macklin, J. D. Kmetec, and C. L. Gordon III, Phys. Rev. Lett. **70**, 766 (1993).
[10] A. L'Huillier and Ph. Balcou, Phys. Rev. Lett. **70**, 774 (1993).
[11] B. Yang, K. J. Schafer, B. Walker, K. C. Kulander, P. Agostini, and L. F. DiMauro, Phys. Rev. Lett. **71**, 3770 (1993).
[12] G. G. Paulus, W. Nicklich, and H. Walther, Europhys. Lett. **27**, 267 (1994).
[13] P. Colosimo, G. Doumy, C. I. Blaga, J. Wheeler, C. Hauri, F. Catoire, J. Tate, R. Chirla, A. M. March, G. G. Paulus, H. G. Muller, P. Agostini, and L. F. DiMauro, Nat. Phys. **4**, 386 (2008).
[14] S. Ghimire, A. D. DiChiara, E. Sistrunk, P. Agostini, L. F. DiMauro, and D. A. Reis, Nat. Phys. **7**, 138 (2011).
[15] O. Schubert, M. Hohenleutner, F. Langer, B. Urbanek, C. Lange, U. Huttner, D. Golde, T. Meier, M. Kira, S. W. Koch, and R. Huber, Nat. Photonics **8**, 119 (2014).
[16] A. Belsky, P. Martin, H. Bachau, A. N. Vasil'ev, B. N. Yatsenko, S. Guizard, G. Geoffroy, and G. Petite, Europhys. Lett. **67**, 301 (2004).
[17] H. Bachau, A. N. Belsky, I. B. Bogatyrev, J. Gaudin, G. Geoffroy, S. Guizard, P. Martin, Yu. V. Popov, A. N. Vasil'ev, and B. N. Yatsenko, Appl. Phys. A **98**, 679 (2010).
[18] P. Daguzan, S. Guizard, K. Krastev, P. Martin, G. Petite, A. Dos Santos, and A. Antonetti, Phys. Rev. Lett. **73**, 2352 (1994).
[19] A. N. Belsky, H. Bachau, J. Gaudin, G. Geoffroy, S. Guizard, P. Martin, G. Petite, A. Philippov, A. N. Vasil'ev, and B. N. Yatsenko, Appl. Phys. B **78**, 989 (2004).
[20] H. Bachau, A. N. Belsky, P. Martin, A. N. Vasil'ev, and B. N. Yatsenko, Phys. Rev. B **74**, 235215 (2006).
[21] R. Numico, D. Giulietti, L. A. Gizzi, and L. Roso, J. Phys. B **33**, 2605 (2000).
[22] L. B. Madsen, Phys. Rev. A **65**, 053417 (2002).
[23] F. Catoire and H. Bachau, Phys. Rev. A **85**, 023422 (2012).
[24] L. V. Keldysh, Sov. Phys. JETP **20**, 1307 (1965).
[25] J. B. Krieger and G. J. Iafrate, Phys. Rev. B **33**, 5494 (1986).
[26] H. N. Nazareno and J. C. Gallardo, Phys. Status Solidi B **153**, 179 (1989).
[27] F. Bloch, Z. Phys. **52**, 555 (1928).
[28] C. Kittel, *Quantum Theory of Solids* (Wiley, New York, 1963).
[29] C. Zener, Proc. R. Soc. A **145**, 523 (1934).